Synergistic apoptosis in head and neck squamous cell carcinoma cells by co-inhibition of insulin-like growth factor-1 receptor signaling and compensatory signaling pathways

Authors: Mark J. Axelrod, PhD[1,2]; Rolando E. Mendez, BS[2]; Ashraf Khalil, MD, PhD[2]; Stephanie S. Leimgruber, MS[3]; Elizabeth R. Sharlow, PhD[3]; Brian Capaldo, BS[4]; Mark Conaway, PhD[5]; Daniel G. Gioeli, PhD[1]; Michael J. Weber, PhD[1]; Mark J. Jameson, MD, PhD[2]

Author Affiliations: University of Virginia Health System, Charlottesville, VA: [1]Department of Microbiology, Immunology, and Cancer Biology; [2]Department of Otolaryngology – Head and Neck Surgery; [3]Department of Pharmacology; [4]Department of Biochemistry and Molecular Genetics; [5]Department of Health Evaluation Sciences

Acknowledgements: The study was supported by NIH grant K08-DE019477 (Jameson), NIH grant P30-CA044579 (Weber), a grant from the Melanoma Research Alliance (Weber), a grant from the James and Rebecca Craig Foundation (Weber), and a UVA Pilot Project Grant (Jameson/Gioeli) funded by the UVA Cancer Center and the UVA Department of Otolaryngology – Head and Neck Surgery.

Corresponding Author Information: Mark J. Jameson, MD, PhD, Division of Head and Neck Surgical Oncology, Department of Otolaryngology – Head and Neck Surgery,

University of Virginia Health System, P O Box 800713, Charlottesville, VA 22908-0713. Tel: 1 434 924 2040. Fax: 1 434 982 3965. E-mail: mark.jameson@virginia.edu.

Running Title: Discovery of synergistic targeted inhibitors for head and neck cancer

Key Words: insulin-like growth factor-1 receptor, head and neck squamous cell carcinoma, drug resistance, compensatory signaling, combination therapy

Abstract

Background: In head and neck squamous cell carcinoma (HNSCC), resistance to single agent targeted therapy may be overcome by co-targeting of compensatory signaling pathways.

Methods: A targeted drug screen with 120 combinations was used on 9 HNSCC cell lines.

Results: Multiple novel drug combinations demonstrated synergistic growth inhibition. Combining the insulin-like growth factor-1 receptor (IGF1R) inhibitor BMS754807 with either the HER-family inhibitor BMS599626 or the Src-family kinase inhibitor dasatinib resulted in substantial synergy and growth inhibition. Depending on the cell line, these combinations induced synergistic or additive apoptosis; when synergistic apoptosis was observed, AKT phosphorylation was inhibited to a greater extent than either drug alone. Conversely, when additive apoptosis occurred, AKT phosphorylation was not reduced by the drug combination.

Conclusions: Combined IGF1R/HER family and IGF1R/Src family inhibition may have therapeutic potential in HNSCC. AKT may be a node of convergence between IGF1R signaling and pathways that compensate for IGF1R inhibition.

Introduction

Despite their promise, targeted cancer therapies used in isolation rarely produce complete or durable responses and usually do not substantially prolong patient survival. When a targeted drug causes robust tumor regression, recurrent tumors that are often more aggressive than the original and refractory to the targeted therapy almost invariably occur.[1] In some cases this is due to the selection of mutations that render the protein target insensitive to the drug. However, even when a drug effectively inhibits an oncogenic driver protein, adaptive survival responses can blunt the cytotoxic effects of the drug, resulting in either intrinsic or acquired resistance.[2] For example, mutations in PIK3CA provide compensatory signaling in 5% of lung cancers that develop resistance to epidermal growth factor receptor (EGFR) tyrosine kinase inhibitors,[3] while BRAF mutations cause resistance in another 1% of tumors.[4]

Signaling proteins involved in these compensatory responses need not be mutationally activated; loss of feedback loops in response to drug treatment may be sufficient to cause aberrant cell signaling leading to drug resistance.[5] Therefore, purely genetic approaches may be ineffective at completely elucidating the mechanisms of drug resistance. Chandarlapaty *et al.* demonstrated that inhibition of AKT in multiple tumor types, including breast and prostate cancers, results in increased expression and phosphorylation of multiple receptor tyrosine kinases (RTKs) including HER3, with associated resistance to AKT inhibitors.[6] In head and neck squamous cell carcinoma (HNSCC), we demonstrated that activation of the insulin-like growth factor-1 receptor (IGF1R) can result in resistance to targeted EGFR inhibitors.[7] Co-targeting components of these adaptive cellular responses in conjunction with the primary therapy can

overcome this resistance and lead to an enhanced cytotoxic effect.[8,9] For example, concurrent inhibition of AKT and HER-family proteins resulted in enhanced growth inhibition of tumors resistant to AKT inhibition via compensatory HER-family activation.[6] The development of strategies to overcome these adaptive compensatory responses to targeted cancer therapies represents an important area for study in order to improve care of cancer patients.

The IGF1R is a membrane-bound RTK comprised of an $(\alpha\beta)_2$ heterotetramer. IGF1R activation, which is initiated by the binding of insulin-like growth factor (IGF)-1 or IGF-2, results in IGF1R auto-phosphorylation as well as phosphorylation of the insulin receptor substrate (IRS) proteins and other targets, ultimately leading to the activation of signaling pathways such as the mitogen activated protein kinase (MAPK) and phosphoinositol-3-kinase (PI3K) pathways. Increased signaling through these pathways results in enhanced proliferation and protection from apoptosis. The IGF1R is a target for therapeutic intervention given its promitotic and prosurvival signaling, as well as its overexpression in a wide range of human cancers.[10] Inhibitors of IGF1R activity have been developed including monoclonal antibodies targeting the ligand binding domain, tyrosine kinase inhibitors, and ligand-neutralizing antibodies against IGF-1 and IGF-2.[11] While clinical studies are ongoing, the results thus far do not indicate that these strategies will be as successful as the preclinical data suggested.

The disappointing clinical outcomes of IGF1R-targted therapies are consistent with the results obtained from other targeted therapies used as single agents in solid tumors. Therefore, it is likely that the maximal benefits of IGF1R-targeted therapies will occur in the context of combinatorial therapies. In order to guide the rational design of

efficacious drug combinations, we have developed a high throughput combinatorial screening methodology that functionally identifies compensatory targets. In previous studies, we validated the ability of this approach to identify drug combinations that result in synergistic growth inhibition.[12–14] The search for synergism between two drugs, rather than simply an augmentation of a single drug response, is a unique element of this approach. Synergistic interactions are indicative of links between the targeted pathways and thus provide insight into compensatory relationships. This knowledge can be applied in two ways to negate resistance: 1) blockade of the compensatory pathway should prevent resistance and/or sensitize cells to inhibition of the primary driver and 2) identification of nodes of convergence between the two pathways can provide new targets for therapeutic intervention that may result in more complete and durable responses.[15] While resistance to combined targeted therapy can occur, it may be less likely to develop when the combination blocks the predicted compensatory pathways, which our drug screen identifies. In the present study, we utilized this combinatorial screening approach to identify drugs that can partner with inhibitors of the IGF1R/PI3K/AKT signaling axis to generate synergistic growth inhibition in HNSCC.

Materials and Methods

Reagents: des[1-3]IGF-1 and recombinant human EGF were obtained from Cell Sciences (Canton, MA). AlamarBlue®, DMEM/F-12 media with HEPES, RPMI 1640 media, and fetal bovine serum were obtained from Invitrogen (Carlsbad, CA). Hydrocortisone was purchased from Sigma-Aldrich (St. Louis, MO). OSI-906 and BMS754807 were obtained from Chemietek (Indianapolis, IN). Gefitinib, lapatinib, crizotinib, and

cederanib were obtained from LC Laboratories (Woburn, MA). Dasatinib, BMS599626, NVP-BEZ235, PF-04691502, XL-147, MK2206, GSK690693, temsirolimus, AT7867, foretinib, panobinostat, SAHA, diclofenac, serdemetan and YM-155 were obtained from Selleck Chemicals (Houston, TX). PF-4708671 was obtained from Santa Cruz Biotechnology (Dallas, TX). PP242 was kindly provided by Dr. Michael Harding (University of Virginia, Charlottesville, VA). Anti-IGF1Rβ, anti-AKT, anti-pAKT (S473), anti-pAKT (T308), anti-EGFR, anti-pEGFR, were obtained from Cell Signaling Technology (Beverly, MA). Anti-pIGF1R/pIR (Y1158/Y1162/Y1163) was obtained from Millipore (Billerica, MA).

Tissue Culture: SCC25, SCC9, Cal27, and FaDu cells obtained from ATCC (Manassas, VA). SCC61, UNC7 and UNC10 cells were kindly provided by Dr. Wendell Yarbrough (Vanderbilt University, Nashville, TN). OSC19 cells were kindly provided by Dr. Jeffrey Myers (The University of Texas MD Anderson Cancer Center, Houston, TX). SCC25GR1 were generated through chronic exposure of SCC25 cells to 5 μM gefitinib in the Jameson lab. Cell line identities were confirmed by DNA fingerprinting (University of Arizona). All cells were grown in DMEM/F-12 media supplemented with 5% FBS and 400ng/mL hydrocortisone and maintained in a 37°C humidified incubator with 5% CO_2. All cell lines were routinely tested and found to be free of mycoplasma contamination using MycoAlert (Lonza, Allendale, NJ).

Growth Assay: 96-well plates were seeded with 3000 - 5000 cells/well in RPMI 1640 supplemented with 0.5% FBS and allowed to adhere overnight. Cells were then treated with inhibitors for 72 h. Cells were incubated with AlamarBlue for 4 h per manufacturer's instructions. Fluorescence at 540 nm was then read on a Synergy2

fluorescence plate reader (Biotek, Winooski, VT). Relative growth inhibition was determined by comparison of drug treated wells against control wells.

Flow Cytometry: 3.75 x 10^5 cells were plated in 60 mm plates in DMEM/F-12 media supplemented with 5% FBS and 400 ng/mL hydrocortisone and allowed to adhere overnight. The media was then replaced with RPMI1640 + 0.5% FBS containing either vehicle or drug. Cells were incubated for either 24 or 72 h followed by collection and staining as previously described.[13] Apoptosis was assessed by a cleaved caspase 3 primary antibody (Cell Signaling) and an anti-rabbit secondary antibody conjugated to phycoerythrin (PE) (Santa Cruz). Samples were analyzed on a FACSCalibur Benchtop Analyzer (Becton Dickenson/Cytek, Fremont, CA) running FlowJo Collectors Edition software (Treestar, Ashland, OR).

Cell Lysis and Western blotting: 3.75 x 10^5 cells were plated in 60 mm plates in DMEM/F-12 media supplemented with 5% FBS and 400 ng/mL hydrocortisone and allowed to adhere overnight. The media was then replaced with RPMI1640 + 0.5% FBS containing either vehicle or drug. Cells were incubated for either 1 h or 24 h. The medium was then aspirated off and the cells were washed for 30 s with ice-cold PBS containing 1 μM pervanadate and 5 nM Calyculin A. The PBS was removed and cells were lysed using a mixture of 1:1 T-PER Tissue Protein Extraction Reagent (Thermo Scientific, Rockford, IL) and 2x Laemmli buffer containing 1 mM phenylmethylsulphonyl fluoride (PMSF), 2 mM pervanadate, 100 μM benzamidine, 1 μg/mL aprotinin, 2 μM pepstatin and 25 μM leupeptin. The lysates were sonicated for 10 minutes in a Bioruptor ice-bath sonicator (Diagenode, Denville, NJ) at maximum output. The lysates were then centrifuged at 13,000 g for 15 min. Western blotting was carried

out as previously described.[16] Immunoblots were analyzed using the Odyssey (LICOR Biosciences, Lincoln, NE) imaging system.

Drug Screen: 96-well plates (Corning Life Sciences / Costar, Corning, NY) were seeded with 3000 - 5000 cells/well in RPMI 1640 supplemented with 0.5% FBS using the FlexDrop Plus Reagent Dispenser (Perkin Elmer, Waltham, MA). The cells were incubated overnight to allow adherence. 96-well drug master plates were prepared by diluting drugs to 10X concentrations in RPMI 1640 + 0.5% FBS. 10X drugs were transferred to cell plates at a final concentration of 1X using the Vprep Automated Liquid Handler (Agilent Technologies, Santa Clara, CA). Cells were incubated for 72 h. AlamarBlue was added using the Vprep to a final concentration of 10%, per manufacturer's instructions. Cells were incubated for 4 h and fluorescence was read at Ex560nm/Em590nm using a Molecular Devices M5 plate reader with Stakmax (Sunnyvale, California).

Statistics: For each of the 9 cell lines, and each of the 120 drug combinations, a three-way ANOVA was conducted on the log-transformed cell growth, with factors representing the dose of each drug in the combination and a factor to account for experiment-to-experiment variation in cell growth. The 3-way ANOVA model included all main effects and 2-way interactions, but no 3-way interaction between experiment and the doses of the two drugs in the combination. This model allows for an estimate, a standard error and a test of statistical significance for the difference between the observed cytotoxicity and the Bliss predicted cytotoxicity. Within each cell line, the combinations were ranked by the estimated degree of % synergy. Unsupervised hierarchal clustering of

maximum synergies across drug combinations and cell lines using Euclidean distance as the similarity metric and average linkage within the R packages gplots[17] and pvclust.[18]

Results

Combination screening identifies drug pairs that cause synergistic growth inhibition in HNSCC. To identify druggable targets that enhance the effects of IGF1R pathway inhibition, we performed a combinatorial drug screen in nine human papilloma virus (HPV)-negative HNSCC cell lines. As shown in Table 1, the inhibitor library was comprised of compounds that are FDA-approved for clinical use (36%, 8 of 22 compounds), are currently in clinical trials (55%, 12 of 22 compounds), or have demonstrated anti-tumor efficacy in *in vivo* model systems (9%, 2 of 22 compounds). We screened 10 IGF1R pathway inhibitors in combination with 12 inhibitors of other targets demonstrated to play important roles in the survival and proliferation of HNSCC cells for a total of 120 drug combinations. Drug concentrations were selected based on dose response experiments performed in all nine cell lines. Doses that produced approximately 10%, 25%, and 40% growth inhibition were selected for screening. For each combination in each cell line, we assessed the growth inhibition caused by each drug alone as well as nine dose combinations (three concentrations of drug A combined with three concentrations of drug B). These results were then compared to a predicted additive growth inhibition that was generated using the Bliss model of additivity[19] to determine whether the drug interaction was synergistic, additive, or subadditive. From this analysis, we generated what we refer to as the "maximum % synergy" value, which is the greatest difference between the actual observed growth inhibition and the Bliss

predicted growth inhibition for a given drug combination in a given cell line. We performed unsupervised hierarchical clustering using the maximum % synergy for each drug combination in each cell in order to observe patterns of response (Figure 1A). This clustering analysis revealed no two cell lines responded similarly to the combination panel ($p > .05$), underscoring the diversity of possible adaptive responses in HNSCC. Additionally, this analysis demonstrated that robust synergies were rarely observed, implying that, when synergistic effects occurred, they were the result of specific pathway interactions rather than being due to non-specific toxicities. To identify drug combinations suitable for further analysis, we generated a histogram using maximum % synergy for each drug combination and cell line (Figure 1B). We focused on combinations with synergistic effects above the 90th percentile, which resulted in a cutoff point at 17% synergy. Table 2 identifies the 25 most synergistic combinations in the screen. This list includes several drug combinations that have not been previously tested in HNSCC and some with targets that would not be anticipated to interact; these may well represent previously unknown compensatory interactions that can contribute to drug resistance. Within this subset of drug combinations, we selected two for further study: BMS754807 combined with dasatinib and BMS754807 combined with BMS599626 (Figure 1C; see below for details) based on the robust synergies and overall growth inhibition generated by these two combinations, as well as their potential near-term clinical application.

The combination of the IGF1R antagonist BMS754807 and the multi-kinase inhibitor dasatinib produced robust synergy in eight of the nine (89%) cell lines tested (Figure 2A). The synergies in these 8 cell lines ranged from 19% to 44%. Additionally,

the overall growth inhibition generated by the combination ranged from 49% to 83%. Further studies with BMS754807 and dasatinib were performed in Cal27 and SCC9 cells, due to the high degree of growth inhibition and robust synergy produced by this combination in these cell lines (Figure 2A). Further analysis of the screening data in these two lines revealed that high degrees of synergy and growth inhibition were observed at all nine dose combinations (1.88 μM, 938 nM, and 469 nM BMS754807 combined with 50 nM, 25 nM, and 12.5 nM dasatinib) of the 3x3 combination matrix (Figure 2B-2C). We also chose to study in more detail the combination of BMS754807 and the HER-family antagonist BMS599626. This decision was based on the high degree of growth inhibition (59%-89%; Figure 2D) and on previous data from our lab indicating that IGF1R is a resistance factor that can mitigate the growth-inhibitory effects of HER family inhibitors.[7] Both the UNC7 and UNC10 cell lines displayed a robust "% synergy" value of greater than 20% in response to treatment with this combination, while the other seven cell lines displayed additive to synergistic interactions and overall growth inhibition greater than 50% (Figure 2D). Both of these cell lines also displayed either additivity or synergy at all nine dose combinations (1.88 μM, 938 nM, and 469 nM BMS754807 combined with 10 μM, 5 μM, and 2.5 μM BMS599626) of the 3x3 combination matrix used in the screen (Figure 2E-2F).

Pharmacophore substitution and pharmacodynamic analysis verifies the drug targets. As in our previous study,[13] we have taken a two-part approach to assuring that the observed biological effects are a consequence of inhibiting the putative targets of the drugs: 1) demonstrate similar synergy and growth inhibition using alternate drugs with the same putative target but a different chemical structure and likely different off-target

effects; and 2) demonstrate inhibition of the putative molecular target at concentrations that result in synergistic growth inhibition. To assess whether the putative targets of these drugs are responsible for the observed synergistic growth inhibition, we performed drug substitution experiments for each of the three drugs. In combination with dasatinib, the IGF1R inhibitor linsitinib (OSI-906) produced synergistic growth inhibition in both SCC9 cells (Figure 3A) and Cal27 cells (not shown). Linsitinib also effectively substituted for BMS754807 in combination with BMS599626 in UNC7 cells (Figure 3B) and UNC10 cells (not shown). Inhibition of Src autophosphorylation by dasatinib has been shown to occur at concentrations which caused synergistic growth inhibition in our screen.[20] In addition, combined inhibition of Src and IGF1R has been reported to be synergistic in a prostate cancer model.[21] To investigate whether inhibition of Src family kinases (SFKs) is necessary for the synergistic effect, we chose saracatinib (AZD-0530) as a substitute for dasatinib. Both compounds inhibit kinases other than SFKs, however the two lists of targets share little overlap other than SFKs.[22,23] Saracatinib was able to successfully substitute for dasatinib in SCC9 cells (Figure 3A) and Cal27 cells (not shown), implicating SFKs as the relevant target critical for synergy. As a substitute for BMS599626, we chose the HER-family inhibitor lapatinib. In combination with BMS754807, lapatinib generated synergy in UNC7 cells (Figure 3B) and enhanced growth inhibition in UNC10 (not shown), indicating that inhibition of HER-family members is necessary for the synergistic effects of the combination. We next tested whether concentrations of each inhibitor that caused synergistic cytotoxicity could inhibit their putative targets. Treatment with 1.875 μM BMS754807 inhibited auto-phosphorylation of the IGF1R upon stimulation with des[1-3]IGF-1 for five minutes

(Figure 3C). We next tested whether dasatinib could inhibit Src autophosphorylation under conditions where we observed synergy. Treatment with 50 nM dasatinib for one hour inhibited basal Src autophosphorylation (Figure 3D). These data indicate that the concentrations of BMS754807 and dasatinib that cause synergistic growth inhibition are in the range that inhibits their respective putative molecular targets. Similarly, cells stimulated with epidermal growth factor (EGF) display robust EGFR phosphorylation, which was fully inhibited by treatment with 10 μM BMS599626 (Figure 3E), again indicating that the concentrations at which BMS754807 and BMS599626 cause synergistic growth inhibition fall within the range where the putative targets are inhibited.

Synergistic growth inhibition is mediated by apoptosis. We used flow cytometry to determine whether combination treatment induced apoptotic cell death. Cal27 and SCC9 cells were treated with vehicle, BMS754807, dasatinib, or the combination for 24 hours. Apoptosis was then assessed by staining for cleaved caspase 3. In Cal27 cells, treatment with BMS754807 and dasatinib as single agents resulted in 5% and 8% cleaved caspase 3 positive cells, respectively. The combination produced 42% caspase 3 positive cells, a robust and synergistic apoptotic response compared to the Bliss prediction of 13% (Figure 4A and 4C). Similar results were observed when the cells were stained with an antibody specific for cleaved PARP (data not shown). SCC9 cells responded similarly to Cal27 cells in both the single drug and combination drug treatment conditions. Treatment with BMS754807 and dasatinib as single agents for 24 hours resulted in 3.5% and 7% of cells staining positive for cleaved caspase 3, respectively. The combination treatment resulted in synergistic apoptosis, with 60% cleaved caspase 3 positive cells compared to a Bliss predicted value of 9% (Figure 4B and 4D).

To assess the apoptotic response to the combination of BMS754807 and BMS599626, we treated UNC7 and UNC10 cells with each drug singly or in combination for 72 hours. Treatment of UNC7 cells with BMS754807 and BMS599626 as single agents resulted in 10% and 44% cleaved caspase 3 positive cells, respectively. The combination displayed a synergistic apoptotic effect, with over 75% of the population staining positive for caspase 3 cleavage compared to a Bliss predicted value of 50% (Figure 4E and 4G). In UNC10 cells, the combination produced an additive apoptotic benefit. Individual treatment led to apoptosis in 17% (BMS754807) and 21% (BMS599626) of the cells. The combination treatment resulted in 39% apoptosis, with the Bliss model predicting 34% apoptosis (Figure 4F and 4H).

Synergistic inhibition of AKT phosphorylation correlates with synergistic apoptosis. Previous work has identified incomplete inhibition of AKT signaling as a possible mechanism allowing HNSCC cells to escape the apoptotic effects of targeted therapeutics [7]. Therefore, we examined the effects that single and combination treatment of HNSCC cells had on AKT phosphorylation (Figure 5A-D). In three of the four cell lines, treatment with BMS754807 resulted in inhibition of AKT phosphorylation. The magnitude of this effect varied between cell lines. However, AKT phosphorylation was not completely inhibited in any of these three cell lines (Figure 5A-C lane 2). In the fourth cell line, UNC10, treatment with BMS754807 had no effect on AKT phosphorylation (Figure 5D lane 2). Cal27 and SCC9 cells treated with dasatinib demonstrated slight reductions in AKT phosphorylation (Figure 5A-B lane 3). Similarly, UNC7 cells treated with BMS599626 had lower levels of AKT phosphorylation than control cells (Figure 5C lane 3). Treatment with a drug combination, however, resulted

in reduction of AKT phosphorylation to near the limits of detection in Cal27, SCC9, and UNC7 cells (Figure 5A-C lane 4); this correlates with the synergistic apoptosis demonstrated in Figure 4. In contrast, the combination did not result in any reduction in AKT phosphorylation in UNC10 cells (Figure 5D lane 4), which also demonstrated only additive and not synergistic apoptosis. These data demonstrate that AKT phosphorylation may be a useful biomarker for therapeutic efficacy and may implicate AKT activity as being a critical survival node in some but not all HNSCC tumors.

Discussion

Unlike standard cytotoxic chemotherapeutic agents, targeted therapies hold the promise of being highly effective with limited toxicity. However, single-agent targeted therapeutics have had little clinical impact on HNSCC and there is thus great interest in identifying combination therapies that might prove more effective. A major confounder of effective treatment by targeted therapies has been the robust compensatory survival responses that occur with single drugs. These responses are often intracellular and autonomous, and can be detected in cell culture, thus providing an opportunity to employ high-throughput technologies that cannot be employed *in vivo*. We[12–14] and others[24] have previously demonstrated that combinatorial drug screening can be used to identify these compensatory responses by detecting drug pairs that cause synergistic cytotoxicity. These studies have been successfully performed in a variety of cancer types, indicating the general utility of such an approach. However, to this point, no such approach has been utilized in HNSCC. It is well established that HNSCC behaves differently from other cancers, even other squamous cell carcinomas such as lung and skin. While some

mechanisms of resistance to targeted therapy have been identified in HNSCC, data regarding compensatory signaling processes are limited. To begin to explore HNSCC compensatory signaling in more detail, we assembled a panel of 9 HNSCC lines and screened them using 120 drug combinations. We were able to identify a number of synergistically inhibitory combinations. Some of these combinations have been previously described, which serves to validate our approach, but many are novel in HNSCC. Interestingly, hierarchical cluster analysis demonstrated enormous heterogeneity in responses to the drug combinations: no two cell lines demonstrated the same pattern of sensitivities. This likely reflects the complex genetic landscape of these tumors, consequent to an etiology of chemical carcinogenesis (e.g. due to tobacco) and local inflammatory reactions.

Despite this heterogeneity, there was a small subset of combinations that produced a robust synergistic response in multiple cell lines. A number of these target combinations have been shown to cause synergistic growth inhibition in other cancer models. For example, we detected synergy using the mTOR inhibitor PP242 and the histone deacetylases (HDAC) inhibitors SAHA and panobinostat. The combination of HDAC and mTOR inhibition has been shown to cause synergistic growth inhibition in gastric cancer[25] and prostate cancer model systems.[26] We also detected synergy using HER-family inhibitors such as lapatinib and BMS599626 in combination with PI3K and AKT inhibitors such as PF-04691502, GSK690693, and MK-2206. Inhibition of EGFR and PI3K/AKT signaling has been shown to be synergistic in many cancer types including breast,[27] ovarian,[28] prostate,[29] and lung.[6] Our ability to detect synergistic co-

targets previously reported in other cancer models, including *in vivo* models, serves as a validation of our screening technique.

Inhibition of IGF1R has been reported to overcome resistance to EGFR inhibitors in a number of cancer models.[30–32] In addition, previous work from our lab has demonstrated that activation of the IGF1R in HNSCC cell lines is protective against apoptosis induced by gefitinib or erlotinib.[7] Consistent with these data, we found that the combination of BMS754807 and BMS599626 resulted in synergistic growth inhibition. We selected this drug combination for further study due to its potentially broad translational applicability to HNSCC and other cancer types.

The other synergistic combination that was selected for follow-up analysis was BMS754807 and dasatinib, a clinically approved multi-kinase inhibitor with activity against SFKs. This combination has been shown to be effective in a pre-clinical model of prostate cancer,[21] but to date has not been reported in HNSCC. This combination caused synergistic growth inhibition in eight of the nine cell lines tested and resulted in a net additive growth inhibition of greater than 75% in the one cell line that did not show synergy. The breadth of the synergistic response to this combination may be indicative of wide-spread efficacy in a clinical setting. Previous work has demonstrated that the Src kinase was able to phosphorylate and activate the IGF1R, independent of IGF1R kinase activity, thus providing a possible mechanistic rationale for combining these two inhibitors.[33]

The first step in understanding the compensatory relationships between the signaling pathways being inhibited was to confirm that the observed growth effects were due to inhibition of the putative targets of the drugs used. ATP-competitive small

molecule inhibitors tend to inhibit the activity of multiple proteins due to similarities in the ATP-binding pockets among kinases.[34] To rule out off-target effects as the main cause of the observed synergies, we confirmed that the putative targets of these drugs were being inhibited at concentrations where synergy occurred in the screen. We also performed drug substitutions using inhibitors with the same putative targets but distinct chemotypes; these alternative compounds have dissimilar off-target effects and are therefore useful for target confirmation. Linsitinib substituted effectively for BMS754807 and lapatinib for BMS599626, confirming that inhibition of the putative targets of BMS754807 and BMS599626, IGF1R and HER-family proteins respectively, are necessary for the observed synergistic growth inhibition. The synergistic impact on cell survival resulting from simultaneous inhibition of both pathways confirms the compensatory relationship between HER family proteins and the IGF1R that has been previously proposed.[7]

In the case of dasatinib, drug substitution with saracatinib recapitulated the synergistic growth inhibition observed in combination with BMS754807 in multiple cell lines. Dasatinib and saracatinib are both potent inhibitors of multiple SFKs. However, dasatinib also potently inhibits a number of EPHA and EPHB family RTKs, as well as other proteins such as Abl, with similar potency to SFKs.[22] Saracatinib, in contrast, displays little inhibitory activity against EPHA and EPHB family members, but does inhibit mutated and wild type EGFR with IC_{50}s comparable to those for the SFKs.[23] Since both inhibitors synergize in combination with IGF1R antagonists, it is likely that their overlapping targets, namely the SFKs, are involved in compensatory signaling

instigated by IGF1R inhibition in these cell lines. However it is also possible that other targets are involved.

The ability of dasatinib to inhibit a range of signaling molecules may give it a therapeutic advantage over similar compounds with more selective targeting. This may also explain why the combination of dasatinib and BMS754807 is synergistic in all but one of the HNSCC cell lines tested, despite their obvious genetic and signaling differences. Although *in vivo* HNSCC model systems are beyond the scope of the present study, this combination demonstrated anti-tumor activity in an *in vivo* model of prostate cancer.[21] These data raise the possibility that the pathways inhibited by this combination are fundamentally critical for survival in not only a broad range of HNSCCs, but also in multiple cancer types. Given this potential widespread therapeutic utility, the molecular mechanism(s) of combined BMS754807/dasatinib treatment warrant further investigation.

Although the inhibition of multiple targets raises the specter of a worse side effect profile when used clinically, dasatinib has proven itself to be well tolerated as a single agent. Currently, dasatinib is being tested in clinical trials as part of combination therapy with bevacizumab or erlotinib. Bevacizumab is a vascular endothelial growth factor receptor (VEGFR)-targeting antibody. Erlotinib is an EGFR inhibitor with a profile of off target effects that is significantly more limited than dasatinib. Thus far, these trials have not reported any severe adverse effects, implying that dasatinib combinations are well tolerated, potentially establishing a paradigm for the combination of a pleotropic kinase inhibitor with a more selective agent; such a model could apply to the dasatinib/BMS754807 combination.

Prior work from our lab has demonstrated that the addition of exogenous IGF-1 to HNSCC cells is protective against apoptosis induced by EGFR antagonists. That study demonstrated an inverse correlation between the degree of AKT phosphorylation and the amount of apoptosis that occurred in response to inhibitor treatment [7]. These data imply that AKT activation is a potential mechanism of resistance to treatment with targeted anti-cancer agents in HNSCC. Thus, we anticipated that the degree of apoptosis caused by the drug combinations in the present study would correlate with AKT inhibition. In three of the four cell lines, treatment with combined BMS754807/dasatinib or BMS754807/BMS599626 resulted in near-complete inhibition of AKT phosphorylation, while treatment with individual drugs had much less impact. At the same concentrations, these combinations produced robust and synergistic apoptotic responses. In contrast, UNC10 cells demonstrated no AKT inhibition with the drug combinations, and, while apoptosis was observed under these conditions, the effect of the drug combinations was not synergistic. Taken together, these data suggest that inhibition of AKT may be necessary to achieve synergism and thus may be crucial to eliminating compensatory signaling that occurs with the use of single agent targeted inhibition.

In a prostate cancer model system, BMS754807 and dasatinib were shown to have differing effects on IGF1R-mediated AKT1 and AKT2 phosphorylation.[21] Thus, a more in depth evaluation of relative AKT1/AKT2 inhibition in response to the synergistic drug combinations identified in this study could provide additional mechanistic insight. It is also possible that the variable relationship between AKT phosphorylation and survival in these cell lines is due to intrinsic differences in the way each cell line responds to drug treatment. Given the established genetic diversity found in cancer of the same type, it is

unsurprising that multiple different survival mechanisms exist that cause resistance to single agent treatment.

Resistance to targeted therapies represents a clinically significant problem that is rooted in part in compensatory signaling responses in tumor cells. From a clinical standpoint, there is enormous potential value in identifying and circumventing these responses. This is especially true in the case of HNSCC, where 5-year survival rates for stage III and IV disease remain well below 50% and have improved little over the last several decades despite recent technical improvements in the treatment options available.[35] Combinatorial cancer therapies have the potential to overcome resistance and cause robust and durable patient responses in this difficult disease. Therapeutic combinations are often initially selected by combining two drugs with some efficacy in the hopes of achieving a greater response. While this approach can be effective, resistance can still occur, particularly if the combination does not inhibit the natural compensatory mechanism; it is crucial to identify combinations that counteract compensatory signaling. While clinical resistance can only be detected by empiric testing, our approach of identifying synergistic drugs is one way to more carefully design drug combinations that could be less likely to encounter resistance clinically. We have shown that co-targeting of primary and compensatory signaling has the potential to overcome resistance. Using combinatorial drug screening as a discovery technique, we have identified a number of potential co-targets for use in therapy combined with IGF1R pathway antagonists. We have also shown that two novel drug combinations, BMS754807/BMS599626 and BMS754807/dasatinib, result in robust and synergistic apoptosis. This synergistic apoptotic response correlates with synergistic inhibition of

AKT phosphorylation. Given that all three of these drugs are either FDA approved or currently in clinical trials, the potential exists for the discoveries reported here to be quickly translated into actionable therapeutic strategies.

References

1. Berns K, Bernards R. Understanding resistance to targeted cancer drugs through loss of function genetic screens. *Drug Resistance Updates*. 2012;15(5–6):268-275. doi:10.1016/j.drup.2012.10.002.

2. Shi H, Hugo W, Kong X, et al. Acquired Resistance and Clonal Evolution in Melanoma during BRAF Inhibitor Therapy. *Cancer Discovery*. 2013. doi:10.1158/2159-8290.CD-13-0642.

3. Sequist LV, Waltman BA, Dias-Santagata D, et al. Genotypic and Histological Evolution of Lung Cancers Acquiring Resistance to EGFR Inhibitors. *Science Translational Medicine*. 2011;3(75):75ra26-75ra26. doi:10.1126/scitranslmed.3002003.

4. Ohashi K, Sequist LV, Arcila ME, et al. Lung cancers with acquired resistance to EGFR inhibitors occasionally harbor BRAF gene mutations but lack mutations in KRAS, NRAS, or MEK1. *Proceedings of the National Academy of Sciences*. 2012;109(31):E2127-E2133. doi:10.1073/pnas.1203530109.

5. Chandarlapaty S. Negative Feedback and Adaptive Resistance to the Targeted Therapy of Cancer. *Cancer Discovery*. 2012;2(4):311-319. doi:10.1158/2159-8290.CD-12-0018.

6. Chandarlapaty S, Sawai A, Scaltriti M, et al. AKT Inhibition Relieves Feedback Suppression of Receptor Tyrosine Kinase Expression and Activity. *Cancer Cell*. 2011;19(1):58-71. doi:10.1016/j.ccr.2010.10.031.

7. Jameson MJ, Beckler AD, Taniguchi LE, et al. Activation of the Insulin-like Growth Factor-1 Receptor Induces Resistance to Epidermal Growth Factor Receptor Antagonism in Head and Neck Squamous Carcinoma Cells. *Molecular Cancer Therapeutics*. 2011;10(11):2124 -2134. doi:10.1158/1535-7163.MCT-11-0294.

8. Muranen T, Selfors LM, Worster DT, et al. Inhibition of PI3K/mTOR Leads to Adaptive Resistance in Matrix-Attached Cancer Cells. *Cancer Cell*. 2012;21(2):227-239. doi:10.1016/j.ccr.2011.12.024.

9. Gioeli D, Wunderlich W, Sebolt-Leopold J, et al. Compensatory Pathways Induced by MEK Inhibition Are Effective Drug Targets for Combination Therapy against Castration-Resistant Prostate Cancer. *Molecular Cancer Therapeutics*. 2011. doi:10.1158/1535-7163.MCT-10-1033.

10. Ouban A, Muraca P, Yeatman T, Coppola D. Expression and distribution of insulin-like growth factor-1 receptor in human carcinomas. *Human Pathology*. 2003;34(8):803-808. doi:10.1016/S0046-8177(03)00291-0.

11. Yee D. Insulin-like Growth Factor Receptor Inhibitors: Baby or the Bathwater? *Journal of the National Cancer Institute*. 2012;104(13):975-981. doi:10.1093/jnci/djs258.

12. Roller DG, Axelrod M, Capaldo BJ, et al. Synthetic Lethal Screening with Small-Molecule Inhibitors Provides a Pathway to Rational Combination Therapies for Melanoma. *Molecular Cancer Therapeutics*. 2012;11(11):2505-2515. doi:10.1158/1535-7163.MCT-12-0461.

13. Axelrod M, Gordon V, Conaway M, et al. Combinatorial drug screening identifies compensatory pathway interactions and adaptive resistance mechanisms. *Oncotarget; Vol 4, No 4: April 2013*. 2013. Available at: http://www.impactjournals.com/oncotarget/index.php?journal=oncotarget&page=article&op=view&path%5B%5D=93. Accessed January 1, 2013.

14. Axelrod M, Ou Z, Brett LK, et al. Combinatorial drug screening identifies synergistic co-targeting of Bruton/'s tyrosine kinase and the proteasome in mantle cell lymphoma. *Leukemia*. 2013. Available at: http://dx.doi.org/10.1038/leu.2013.249.

15. Axelrod M, Gordon V, Mendez RE, et al. p70S6 Kinase is a Critical Node of Interaction for Multiple Synergistic Drug Combinations. *Cellular Signaling*. In Press.

16. Gordon V, Bhadel S, Wunderlich W, et al. CDK9 Regulates AR Promoter Selectivity and Cell Growth through Serine 81 Phosphorylation. *Molecular Endocrinology*. 2010;24(12):2267 -2280. doi:10.1210/me.2010-0238.

17. Gregory R. Warnes, Ben Bolker, Lodewijk Bonebakker, et al. gplots: Various R programming tools for plotting data. R package version 2.11.3. 2013.

18. Ryota Suzuki, Hidetoshi Shimodaira. pvclust: Hierarchical Clustering with P-Values via Multiscale Bootstrap Resampling. 2011.

19. Bliss C. The toxicity of poisons applied jointly. *Annals of Applied Biology*. 1939;(26):585-615.

20. Buettner R, Mesa T, Vultur A, Lee F, Jove R. Inhibition of Src Family Kinases with Dasatinib Blocks Migration and Invasion of Human Melanoma Cells. *Molecular Cancer Research*. 2008;6(11):1766-1774. doi:10.1158/1541-7786.MCR-08-0169.

21. Dayyani F, Parikh NU, Varkaris AS, et al. Combined Inhibition of IGF-1R/IR and Src Family Kinases Enhances Antitumor Effects in Prostate Cancer by Decreasing Activated Survival Pathways. *PLoS ONE*. 2012;7(12):e51189. doi:10.1371/journal.pone.0051189.

22. Kitagawa D, Yokota K, Gouda M, et al. Activity-based kinase profiling of approved tyrosine kinase inhibitors. *Genes Cells*. 2013;18(2):110-122. doi:10.1111/gtc.12022.

23. Green TP, Fennell M, Whittaker R, et al. Preclinical anticancer activity of the potent, oral Src inhibitor AZD0530. *Molecular Oncology*. 2009;3(3):248-261. doi:10.1016/j.molonc.2009.01.002.

24. Held MA, Langdon CG, Platt JT, et al. Genotype-Selective Combination Therapies for Melanoma Identified by High-Throughput Drug Screening. *Cancer Discovery*. 2012. doi:10.1158/2159-8290.CD-12-0408.

25. Sun D, Zhang Y, Tian X, Chen Y, Fang J. Inhibition of mTOR signalling potentiates the effects of trichostatin A in human gastric cancer cell lines by promoting histone acetylation. *Cell Biol Int*. 2013.

26. Wedel S, Hudak L, Seibel J-M, et al. Impact of combined HDAC and mTOR inhibition on adhesion, migration and invasion of prostate cancer cells. *Clin Exp Metastasis*. 2011;28(5):479-491. doi:10.1007/s10585-011-9386-8.

27. Yi YW, Hong W, Kang HJ, et al. Inhibition of the PI3K/AKT pathway potentiates cytotoxicity of EGFR kinase inhibitors in triple-negative breast cancer cells. *J Cell Mol Med*. 2013;17(5):648-656. doi:10.1111/jcmm.12046.

28. Glaysher S, Bolton LM, Johnson P, et al. Targeting EGFR and PI3K pathways in ovarian cancer. *Br J Cancer*. 2013;109(7):1786-1794.

29. Festuccia C, Gravina GL, Muzi P, et al. Akt down-modulation induces apoptosis of human prostate cancer cells and synergizes with EGFR tyrosine kinase inhibitors. *Prostate*. 2008;68(9):965-974. doi:10.1002/pros.20757.

30. Morgillo F, Kim W-Y, Kim ES, Ciardiello F, Hong WK, Lee H-Y. Implication of the Insulin-like Growth Factor-IR Pathway in the Resistance of Non–small Cell Lung Cancer Cells to Treatment with Gefitinib. *Clinical Cancer Research*. 2007;13(9):2795-2803. doi:10.1158/1078-0432.CCR-06-2077.

31. Galer CE, Corey CL, Wang Z, et al. Dual inhibition of epidermal growth factor receptor and insulin-like growth factor receptor I: Reduction of angiogenesis and

tumor growth in cutaneous squamous cell carcinoma. *Head Neck*. 2011;33(2):189-198. doi:10.1002/hed.21419.

32. Kim W-Y, Prudkin L, Feng L, et al. Epidermal growth factor receptor and K-Ras mutations and resistance of lung cancer to insulin-like growth factor 1 receptor tyrosine kinase inhibitors. *Cancer*. 2012;118(16):3993-4003. doi:10.1002/cncr.26656.

33. Peterson JE, Jelinek T, Kaleko M, Siddle K, Weber MJ. c phosphorylation and activation of the IGF-I receptor in src-transformed cells. *Journal of Biological Chemistry*. 1994;269(44):27315-27321.

34. Davies SP, Reddy H, Calvano M, Cohen P. Specificity and mechanism of action of some commonly used protein kinase inhibitors. *Biochemical Journal*. 2000;(351):95-105.

35. Cripps C, Winquist E, Devries MC, Stys-Norman D, Gilbert R. Epidermal growth factor receptor targeted therapy in stage III and IV head and neck cancer. *Current Oncology; Vol 17, No 3 (2010)*. 2010. Available at: http://www.current-oncology.com/index.php/oncology/article/view/520/452.

Figure Legends

Figure 1 **– Combinatorial drug screening identifies synergistic co-targets.** A. 120 drug combinations were tested in a panel of nine HNSCC cell lines. The maximum percent synergy was determined for each combination in each cell line as described in *Methods*. Unsupervised hierarchical clustering was performed using the maximum % synergy for each drug combination in each cell line from the screen. Darker green shading indicates greater synergy. B. Maximum % synergy values were plotted and the 90th percentile identified at 17% synergy (denoted by the red box) C. Two drug combinations that caused synergy above the cut-off were selected for further study – BMS754807/dasatinib (red triangles) and BMS754807/BMS599626 (green circles).

Figure 2 – **Synergistic drug combinations were effective in multiple cell lines and over multiple doses.** A. The combination of BMS754807 and dasatinib caused synergistic growth inhibition in eight of the nine cell lines tested and greater than 50% growth inhibition in eight of the nine cell lines tested. B and C. The combination of BMS754807 and dasatinib caused synergistic growth inhibition at multiple dose combinations of a 3x3 dose matrix in Cal27 and SCC9 cells. D. The combination of BMS754807 and BMS599626 caused synergistic growth inhibition in two of the nine cell lines tested and greater than 50% growth inhibition in nine of the nine cell lines tested. E and F. The combination of BMS754807 and BMS599626 caused synergistic growth inhibition at multiple dose combinations of a 3x3 dose matrix in UNC7 and UNC10 cells.

Figure 3 – **Pharmacophore substitutions and target inhibition validate on-target effects.** A and B. Compounds with the same putative targets but distinct chemotypes were substituted for the drugs that initially caused synergy. The original compounds are in bold font. Substitution of linsitinib for BMS754807 or saracatinib for dasatinib maintains synergistic growth inhibition in SCC9 cells (A). Substitution of linsitinib for BMS754807 or lapatinib for BMS599626 maintains synergistic growth inhibition in UNC7 cells (B). C. BMS754807 (1.875 μM) inhibits IGF1R phosphorylation in SCC9 cells. Cells were treated with inhibitor for one hour prior to 10 nM des[1-3]IGF-1 stimulation for 10 minutes. D. Dasatinib (50 nM) inhibits basal Src autophosphorylation in SCC9 cells. E. BMS599626 (10 μM) inhibits EGF stimulated EGFR autophosphorylation in UNC7 cells. Cells were treated with inhibitor for one hour prior to 10 nM EGF stimulation for 5 minutes.

Figure 4 – **Synergistic growth inhibition is mediated by apoptosis.** Apoptosis was assessed by flow cytometric analysis of caspase 3 cleavage. A. Cal27 cells were treated with vehicle (DMSO), 938 nM BMS754807, 25 nM dasatinib, or the combination for 24 hours. B. SCC9 cells were treated with vehicle (DMSO), 469 nM BMS754807, 25 nM dasatinib, or the combination for 24 hours. C. and D. Three independent biological replicates were quantified for each cell line (C. Cal27, D. SCC9). E. UNC7 cells were treated with vehicle (DMSO), 938 nM BMS754807, 5 μM BMS599626, or the combination for 72 hours. F. UNC10 cells were treated with vehicle (DMSO), 469 nM BMS754807, 5 μM BMS599626, or the combination for 72 hours. G. and H. Three independent biological replicates were quantified for each cell line (G. UNC7, H.

UNC10). Error bars represent the standard error of the mean for the three biological replicates. Bliss predicted additive values (white bars) were calculated as described in *Methods*.

Figure 5 – **Synergistic apoptosis is correlated with synergistic inhibition of AKT phosphorylation.** A. Cal27 cells were treated for 24 hours with vehicle (DMSO), 938 nM BMS754807, 25 nM dasatinib, or the combination. B. SCC9 cells were treated for 24 hours with vehicle (DMSO) 469 nM BMS754807, 25 nM dasatinib, or the combination. C. UNC7 cells were treated for 24 hours with vehicle (DMSO), 938 nM BMS754807, 5 μM BMS599626, or the combination. D. UNC10 cells were treated for 24 hours with vehicle (DMSO), 469 nM BMS754807, 5 μM BMS599626, or the combination. All Western blots shown are representative images of three independent biological replicates.

Table 1 – **Compounds used in the combination drug screen.** The 22 compounds used for combinatorial drug screening are listed along with their putative targets and level of clinical development.

Table 2 – **Most synergistic drug combinations.** Drug combinations were rank ordered by % synergy and the 25 most synergistic combinations are shown, along with the cell line in which the synergy occurred.

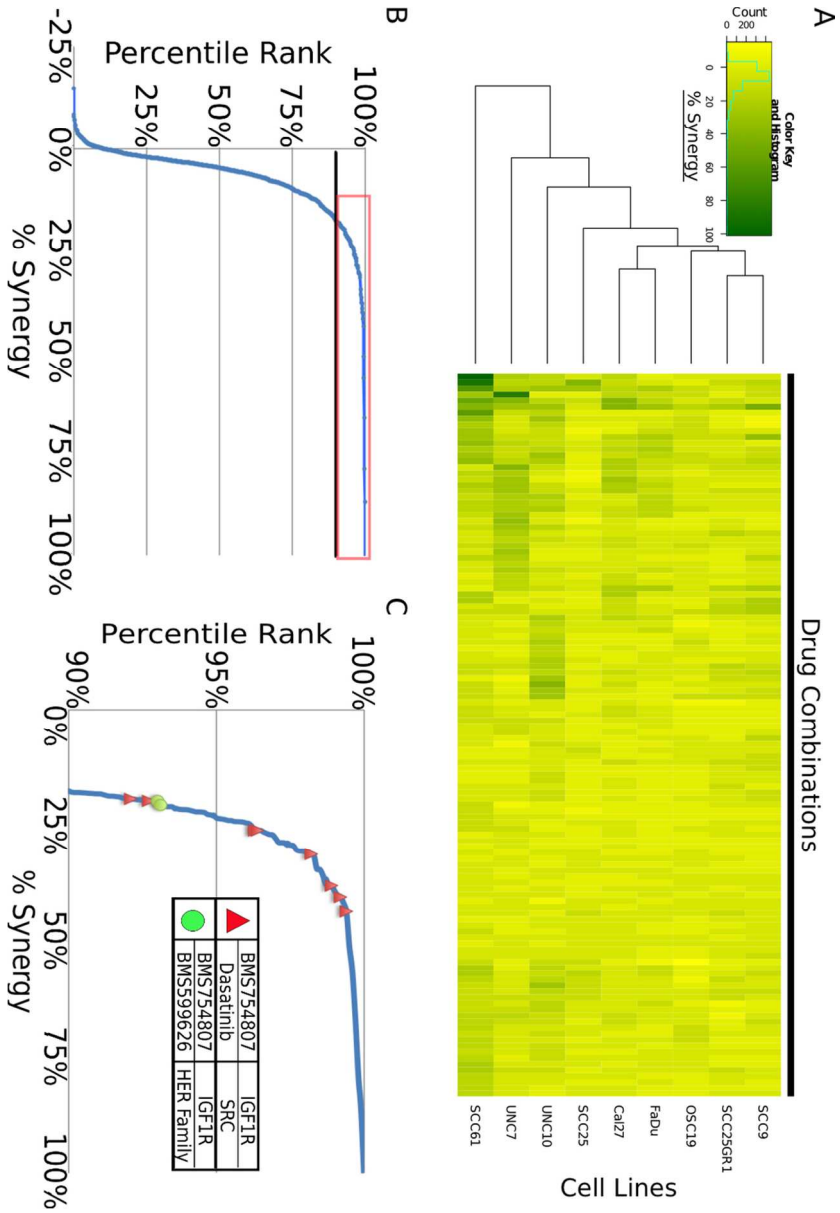

92x134mm (300 x 300 DPI)

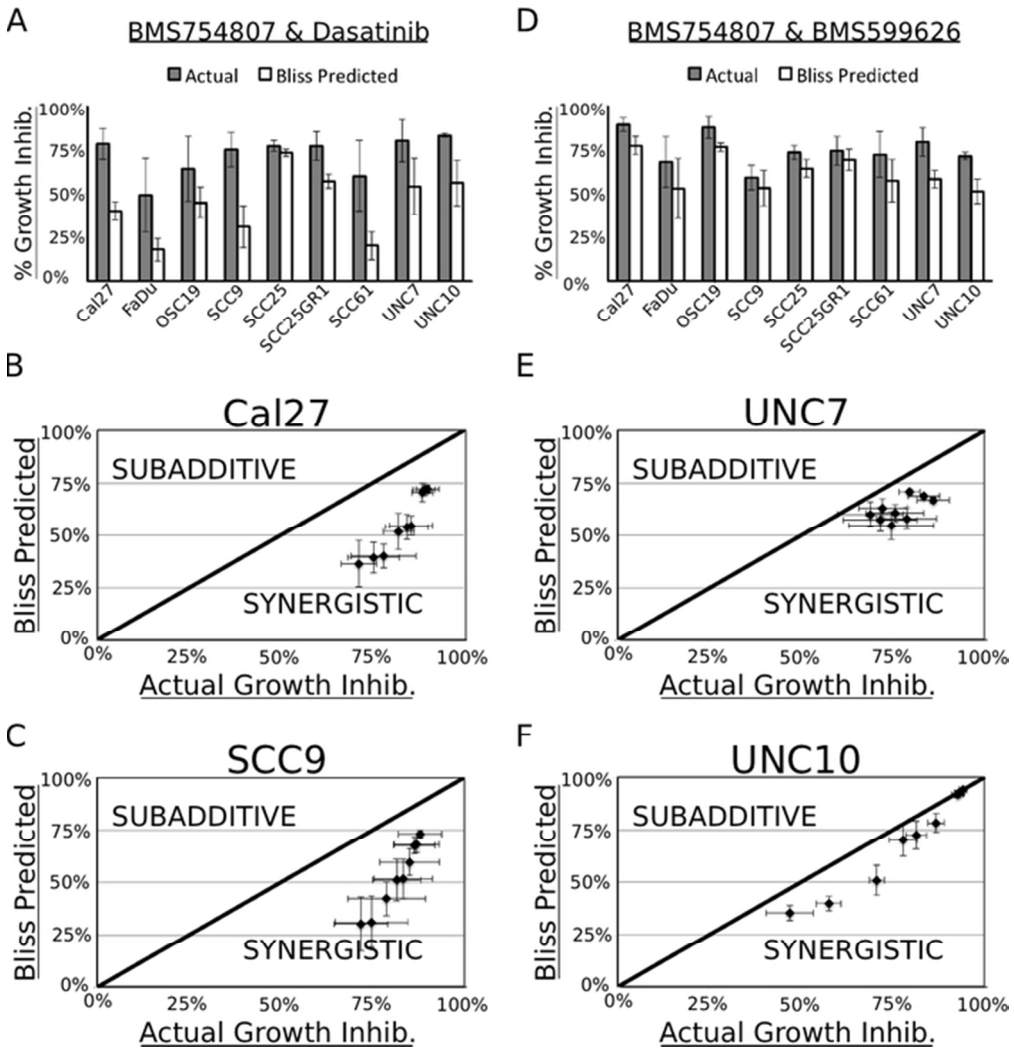

59x61mm (300 x 300 DPI)

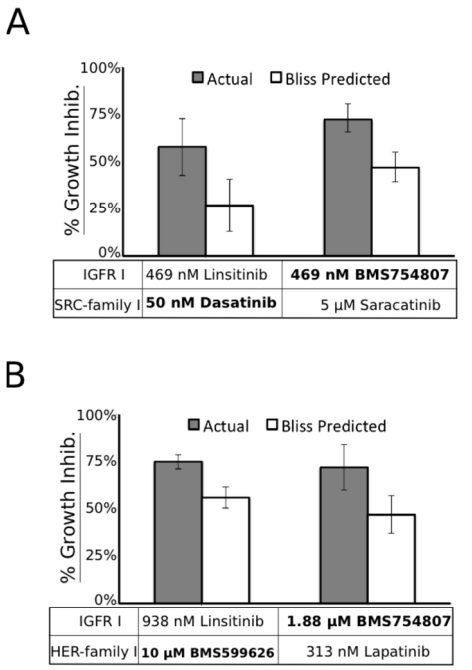

85x222mm (300 x 300 DPI)

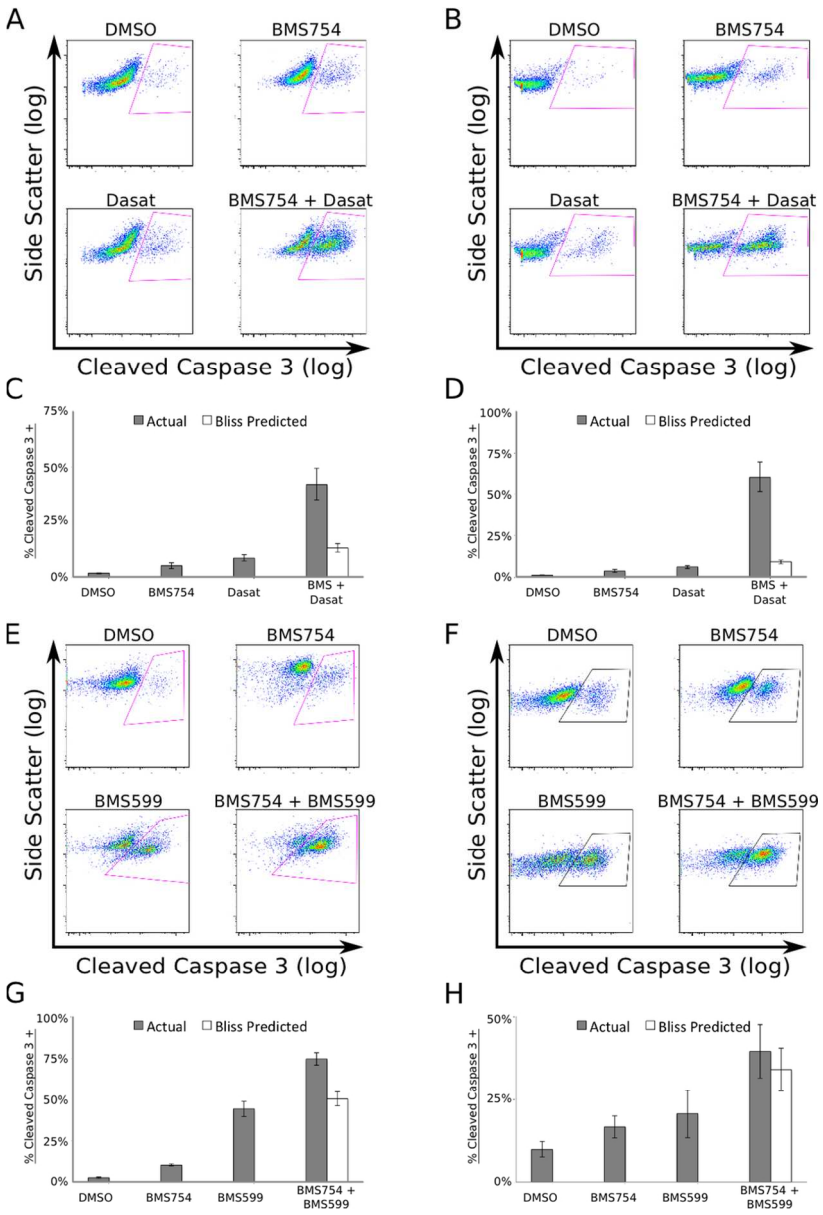

92x137mm (300 x 300 DPI)

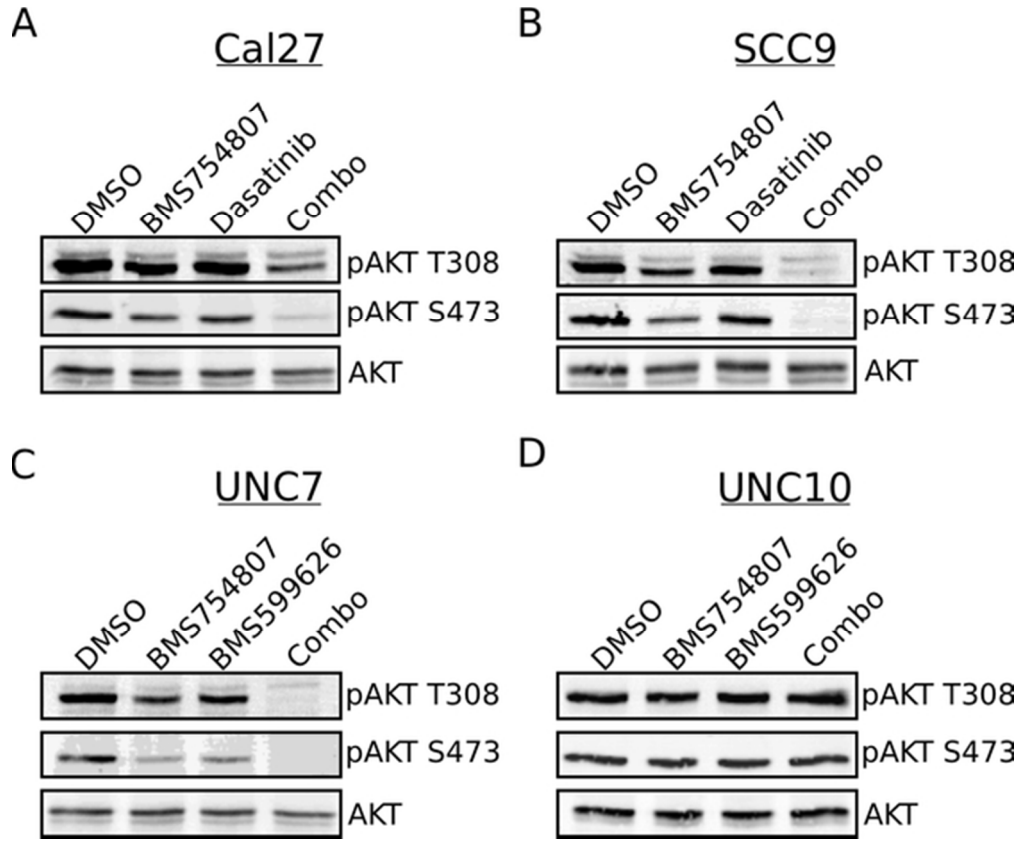

53x44mm (300 x 300 DPI)

Drug	Target	Stage of Development
GSK-690693	AKT	Phase 1
MKK2206	AKT	Phase 2
AT7867	AKT / p70S6K	*In vivo* efficacy
Crizotinib	ALK / MET	FDA approved
Diclofenac	COX	FDA approved
Gefitinib	EGFR	FDA approved
Panobinostat (LBH589)	HDAC	Phase 3
SAHA (vorinostat)	HDAC	FDA approved
Serdametan (JNJ-26854156)	HDM2	Phase 1
BMS599626 (AC480)	HER family	Phase 1
Lapatinib	HER family	FDA approved
BMS754807	IGF1R / InsR	Phase 2
Linsitinib (OSI-906)	IGF1R / InsR	Phase 2
PP242	mTOR	*In vivo* efficacy
Temsirolimus	mTOR	FDA approved
Dasatinib	Multi-kinase including SFKs	FDA approved
XL-147 (SAR245408)	PI3K	Phase 2
NVP-BEZ235	PI3K / mTOR	Phase 2
PF-04691502	PI3K / mTOR	Phase 2
YM155	Survivin	Phase 2
Cederanib	VEGFR	FDA approved
Foretinib (XL880)	VEGFR2 / MET	Phase 2

154x118mm (300 x 300 DPI)

Cell Line	Primary Drug (Target)	Secondary Drug (Target)	% Synergy
UNC7	GSK-690693 (AKT)	Crizotinib (ALK/MET)	40%
SCC61	GSK-690693 (AKT)	Panobinostat (HDAC)	37%
SCC61	MKK2206 (AKT)	Dasatinib (SFKs)	35%
SCC61	AT7867 (AKT/p70S6K)	Crizotinib (ALK/MET)	66%
SCC61	AT7867 (AKT/p70S6K)	Panobinostat (HDAC)	101%
SCC61	AT7867 (AKT/p70S6K)	SAHA (HDAC)	56%
SCC61	AT7867 (AKT/p70S6K)	Serdemetan (HDM2)	35%
SCC25	AT7867 (AKT/p70S6K)	Dasatinib (SFKs)	39%
SCC61	AT7867 (AKT/p70S6K)	Dasatinib (SFKs)	87%
UNC10	AT7867 (AKT/p70S6K)	Foretinib (VEGFR2 / MET)	38%
Cal27	BMS754807 (IGF1R)	Dasatinib (SFKs)	38%
FaDu	BMS754807 (IGF1R)	Dasatinib (SFKs)	31%
SCC61	BMS754807 (IGF1R)	Dasatinib (SFKs)	40%
SCC9	BMS754807 (IGF1R)	Dasatinib (SFKs)	44%
UNC10	BMS754807 (IGF1R)	Foretinib (VEGFR2 / MET)	30%
SCC61	Linsitinib (IGF1R)	Panobinostat (HDAC)	31%
UNC7	Linsitinib (IGF1R)	Panobinostat (HDAC)	79%
UNC7	Linsitinib (IGF1R)	SAHA (HDAC)	36%
SCC61	Linsitinib (IGF1R)	Dasatinib (SFKs)	31%
SCC9	Linsitinib (IGF1R)	Dasatinib (SFKs)	32%
Cal27	PP242 (mTOR)	Panobinostat (HDAC)	38%
SCC61	PP242 (mTOR)	Panobinostat (HDAC)	51%
UNC7	PP242 (mTOR)	Panobinostat (HDAC)	42%
UNC10	PP242 (mTOR)	Foretinib (VEGFR2 / MET)	31%
SCC61	PF-04691502 (PI3K / mTOR)	Dasatinib (SFKs)	31%

176x134mm (300 x 300 DPI)